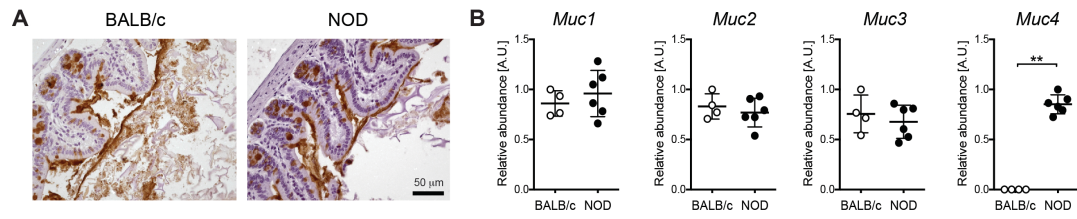
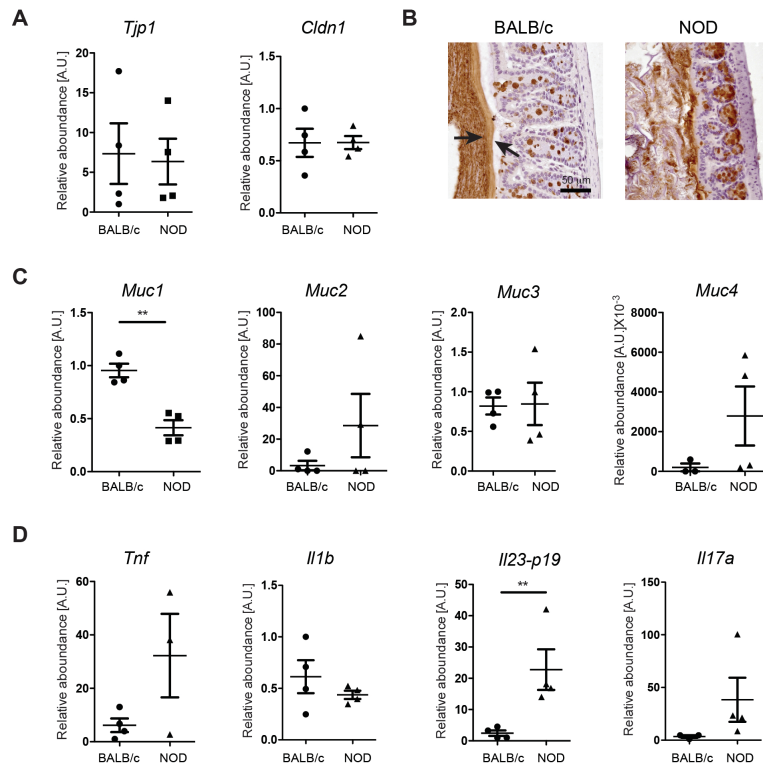


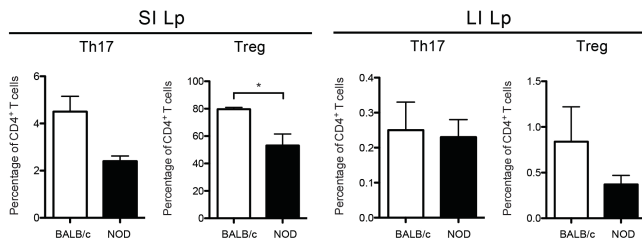
Supplementary Figure 1. **Comparison of gut barrier integrity and intestinal inflammation markers between NOD mice and control C57BL/6 mice.** (A) RT-qPCR analysis of tight junction protein 1 (*Tjp1*) and claudin 1 (*Cldn1*) on tissue homogenates from the colon of 4-6 week-old C57BL/6 and NOD mice. (B) Immunohistochemistry of Muc2 protein in the colon of 4-6 weeks-old NOD mice and C57BL/6 controls. (C) RT-qPCR analysis of *Muc1*, *Muc 2*, *Muc3* and *Muc4* mucin genes in the colon of C57BL/6 and NOD mice. (D) RT-qPCR analysis of cytokine genes encoding TNF- α (*Tnf*), interleukin-1 β (*Il1b*), subunit p19 of IL-23 (*Il23-p19*) and IL-17A (*Il17a*) on tissue homogenates from the colon of 4-6 week-old C57BL/6 and NOD mice.



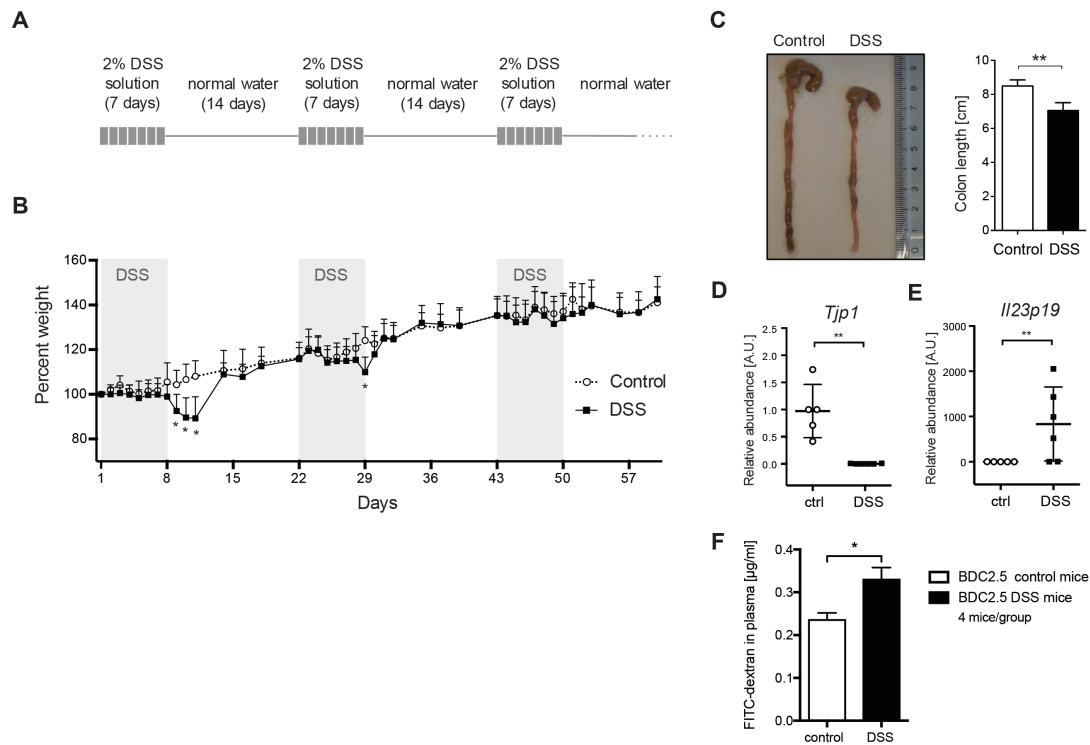
Supplementary Figure 2. **Mucin structure and composition in the small intestine (ileum segment) of NOD and control mice.** (A) Immunohistochemistry of Muc2 protein in the ileum of 4-6 weeks-old NOD mice and Balb/c controls. (B) RT-qPCR analysis of *Muc1*, *Muc 2*, *Muc3* and *Muc4* mucin genes in the ileum of NOD mice and control Balb/c mice.



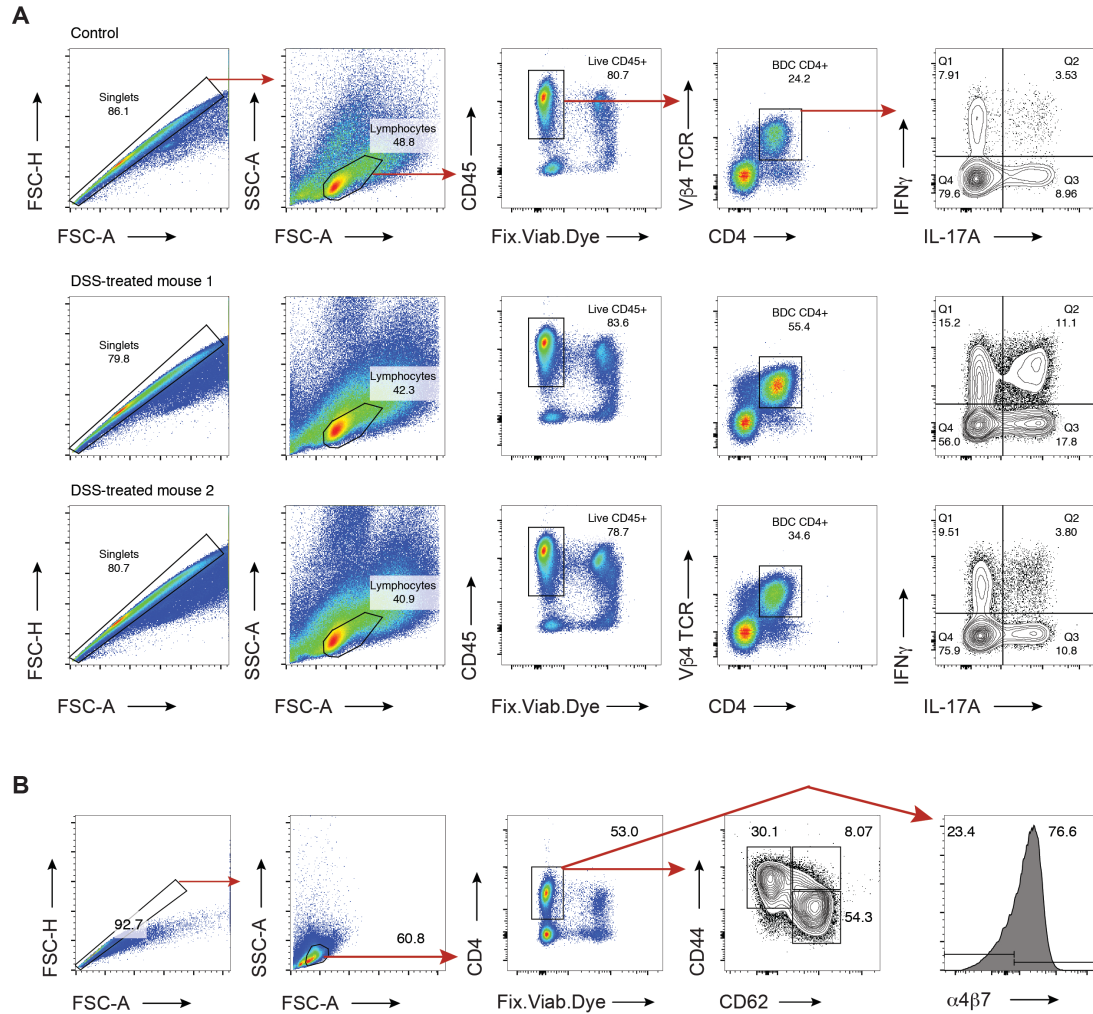
Supplementary Figure 3. **Gut inflammation and alterations of mucus structure and composition in 10-12 week old NOD mice.** (A) Immunohistochemistry of Muc2 protein in the colon of 10-12 weeks-old NOD mice and Balb/c controls. (B) RT-qPCR analysis of tight junction protein 1 (Tjp1) and claudin 1 (Cldn1) on tissue homogenates from the colon of 10-12 week-old BALB/c and NOD mice. (C) (D) RT-qPCR analysis of Muc1, Muc 2, Muc3 and Muc4 mucin genes in the colon of BALB/c and NOD mice. (D) RT-qPCR analysis of cytokine genes encoding TNF- α (Tnf), interleukin-1 β (Il1b), subunit p19 of IL-23 (Il23-p19) and IL-17A (Il17a) on tissue homogenates from the colon of 10-12 week-old BALB/c and NOD mice. * $p < 0.05$, ** $p < 0.01$.



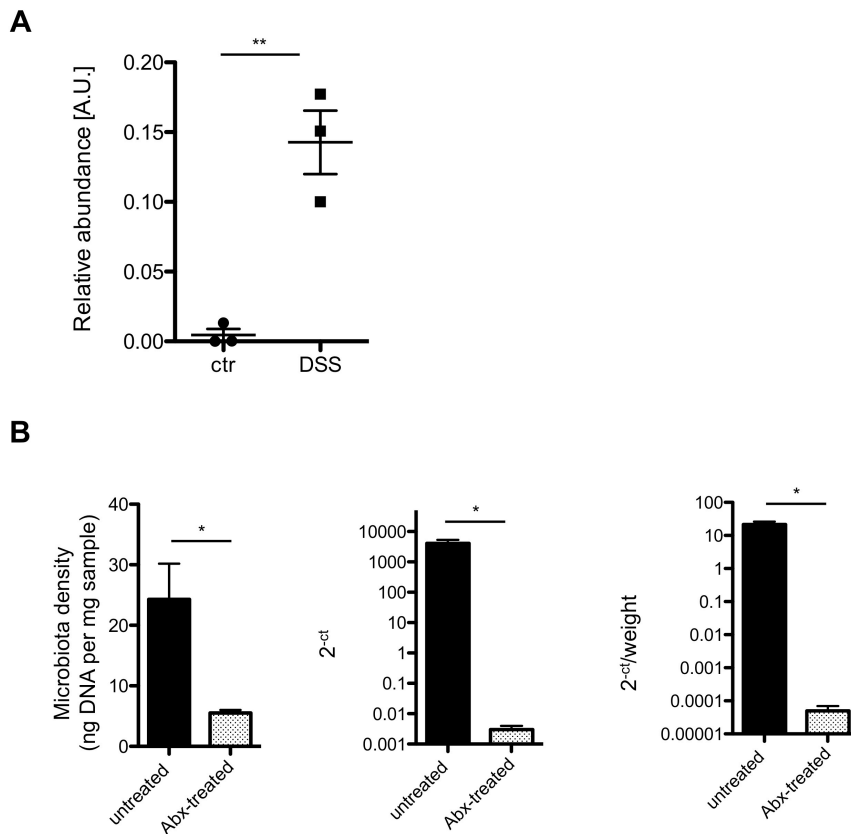
Supplementary Figure 4. **Immunological profiling in the small and large intestinal mucosa of NOD and control mice.** Flow cytometric analysis of Th17 and Treg cells in the small intestinal (SI) and large intestinal (LI) lamina propria (Lp) of 4-6 weeks-old BALB/c and NOD mice. Data are presented as mean percentages \pm SEM of IL-17⁺CD4⁺ and FoxP3⁺CD25⁺CD4⁺ T cells out of total CD4⁺ T cells. * p<0.05.



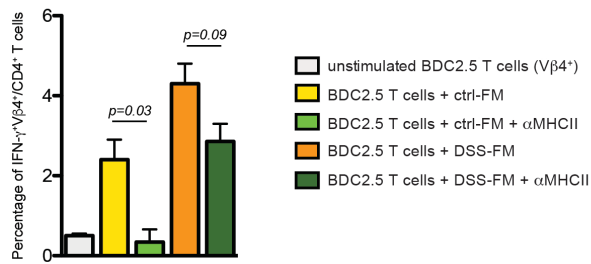
Supplementary Figure 5. **Low-dose DSS administration causes chronic colitis in *BDC2.5XNOD* mice.** (A) Schematic representation of the protocol adopted for the induction of chronic DSS colitis in *BDC2.5XNOD* mice. (B) Body-weight development in *BDC2.5XNOD* mice during repeated administration of DSS-supplemented (*full squares*) or normal drinking water (*open circles*). (C) Representative image (*left panel*) and quantitative evaluation (*right panel*) of colon length in control and DSS-treated *BDC2.5XNOD* mice. (D and E) RT-qPCR analysis of *Tjp1* and *IL-23p19* in colon tissues of control and DSS-treated *BDC2.5XNOD* mice. (F) FITC-dextran *in-vivo* permeability assay showed increased gut permeability in DSS-treated *BDC2.5XNOD* mice (DSS) compared to untreated *BDC2.5XNOD* controls. * $p < 0.05$, ** $p < 0.01$.



Supplementary Figure 6. **Gating strategy for identification and analysis of islet-reactive $V\beta 4^+$ BDC2.5 T cells.** (A) Analysis of cytokine-secretion profile of $V\beta 4^+$ BDC2.5 T cells in the colonic lamina propria. (B) Analysis of the $CD44^{\text{high}}$, $CD62L^{\text{low}}$ activation state of BDC2.5 T cells in the PLN. For intracellular cytokine staining, single cell suspensions isolated from different organs were PMA stimulated in the presence of Brefeldin A, then stained for surface markers, fixed and permeabilized using the BD Cytofix/Cytoperm kit, and finally stained for intracellular cytokines. The following antibodies were used: PerCP-Cy5.5 anti-mouse CD4 (RM4-5, BD Biosciences), APC-eFluor 780 anti-mouse CD45 (30-F11, eBioscience), FITC anti-mouse $V\beta 4$ TCR (KT4, BD Biosciences), APC-Cy7 anti-mouse CD44 (IM7, BD Biosciences), Alexa Fluor 647 anti-mouse CD62L (MEL-14, BioLegend), FITC anti-mouse IFN- γ (XMG-1.2, BD Biosciences), Alexa Fluor 647 or 488 anti-mouse IL-17A (TC11-18H10, BD Biosciences). Dead cells were stained with Fixable Viability Dye eFluor 506 (eBioscience) and excluded from the analysis. Flow cytometry was performed using FACSCanto II (BD Biosciences) and data were analyzed with FCS Express V4 software (De Novo Software).



Supplementary Figure 7. **(A) Bacterial translocation in the mesenteric lymph nodes of DSS-treated BDC2.5XNOD mice.** MLN were isolated from *BDC2.5XNOD* mice either untreated (ctr) or treated with DSS (DSS). MLN were digested with collagenase type IV to obtain a single-cell suspension and host mononuclear cells were removed by centrifugation at $1,900 \times g$ for 10 min and bacterial pellets were collected after centrifugation at $20,000 \times g$ for 10 min according to previously published methods (Obata *et al.* *PNAS* 2010, doi: 10.1073/pnas.1001061107). Total bacterial DNA was isolated from bacterial pellet using PowerFecal-DNA-isolation kit (MioBio) following the manufacturers' instructions. Samples were normalized for DNA content and quantitative PCR analysis for 16s rRNA coding DNA was carried out using a LightCycler 480 (Roche). Primer sequences for universal eubacteria were used as previously described (Atarashi K. *et al.* *Science* 2011) (Fw: GGTGAATACGTTCCCGG Rev: TACGGCTACCTTGTTACGACTT). **(B-D) The antibiotic treatment depleted mice of endogenous microbiota.** 4 week-old mice were treated with the antibiotic cocktail (0.5 g/l vancomycin, 1 g/l ampicillin, 1 g/l metronidazole and 1 g/l neomycin: all from Sigma-Aldrich) for 2 weeks. (B) Microbiota density was calculated as total DNA extracted from each sample (in ng) per mg of fresh fecal sample as previously shown (Contijoch EJ *et al.* *eLife* 2019). (C-D) Total DNA was isolated from fecal pellets using a QIAamp DNA Stool mini kit (QIAGEN). Quantitative PCR analysis was carried out using universal eubacteria primers as in (A) and relative quantities of total microbiota were calculated by the ΔC_t method and normalized to the DNA content (C) or to the weight of fecal sample (D). Data from stool of mice before (untreated) and after treatment with antibiotics (Abx-treated) are shown. * $p < 0.05$, ** $p < 0.01$.



Supplementary Figure 8. **Commensal gut microbiota trigger activation of islet-reactive T cells with a TCR-mediated mechanism.** Fecal material from healthy (ctrlFM) or DSS-colitis (DSSFM) *BDC2.5XNOD* mice was added to splenocytes of TCR tg *BDC2.5XNOD* mice and after 96 h T cell activation was assessed by measuring percentage of V β 4 $^+$ T cells (BDC2.5 T cells) expressing IFN- γ^+ . Monoclonal antibody against murine MHC class II (clone M5/114.15.2) was added at 10 μ g/ml to block TCR-mediated stimulation of BDC2.5 T cells (CD4 $^+$ T cells). Data are presented as mean percentages \pm SEM of IFN- γ^+ V β 4 $^+$ T cells out of total CD4 $^+$ T cells.

Supplementary Table S1

Target gene	Forward primer	Reverse primer
<i>Il1b</i>	CAA CCA ACA AGT GAT ATT CTC CAT G	GAT CCA CAC TCT CCA GCT GCA
<i>Tnfa</i>	TCC ACT TGG TGG TTT GCT ACG	ATG AGC ACA GAA AGC ATG ATC
<i>Il17a</i>	TCA TCC CTC AAA GCT CAG CG	TTC ATT GCG GTG GAG AGT CC
<i>IL23</i>	GTG ACA TGT GGG TTG AGC CT	GGC ATG AGG TTC CGA AAA GC
<i>Tjp1</i>	ACC CGA AAC TGA TGC TGT GGA TAG	AAA TGG CCG GGC AGA ACT TGT GTA
<i>Cldn1</i>	GAT GTG GAT GGC TGT CAT TG	CCT GGC CAA ATT CAT ACC TG
<i>Muc1</i>	TAC CCT ACC TAC CAC ACT CAC G	CTG CTA CTG CCA TTA CCT GC
<i>Muc2</i>	CAC CAA CAC GTC AAA AAT CG	GGT CTC TCG ATC ACC ACC AT
<i>Muc3</i>	CTT CCA GCC TTC CCT AAA CC	TCC ACA GAT CCA TGC AAA AC
<i>Muc4</i>	GAG AGT TCC CTG GCT GTG TC	GGA CAT GGG TGT CTG TGT TG
<i>Rpl32</i>	AAG CGA AAC TGG CGG AAA C	TAA CCG ATG TTG GGC ATC AG
<i>Eubacteria</i>	GGT GAA TAC GTT CCC GG	CCT GTG AAG CGT CAC TGT GT